



Reaction of Pyrrole and Chlorauric Acid

A New Route to Composite Colloids

Matthew C. Henry, Chen-Chan Hsueh, Brian P. Timko, and Michael S. Freund^{a,z}

Department of Chemistry, Lehigh University, Bethlehem, Pennsylvania 18105, USA

Composite colloids of gold and polypyrrole were prepared using two different methods: 1, using pyrrole colloid, created by the oxidation of pyrrole by ferric chloride, to subsequently reduce chlorauric acid and, 2, oxidizing pyrrole monomer with chlorauric acid in a sodium dodecylbenzene sulfonate solution. In each case, the polypyrrole colloid consisted of irregularly shaped particles approximately 500 nm in diameter. The gold produced in each case was in the form of irregular spheres, approximately 407 nm in diameter in method 1 and 13 nm in method 2. X-ray photoelectron spectroscopy was used to determine the oxidation state of the species present. Transmission electron microscopy and light scattering data were used to determine the particle sizes of both gold and polypyrrole colloids. Energy dispersed spectrum X-ray analysis and electron diffraction were used to confirm the presence of metallic gold in the composite colloids. The second-order rate constant for the reaction of chlorauric acid with pyrrole in dilute solution was found to be $13 \text{ M}^{-1} \text{ s}^{-1}$. Aqueous solutions of palladium, platinum, rhodium, cobalt, tin, silver, zinc, nickel, titanium, cadmium, mercury, arsenic, and selenium were also examined for their potential to act as oxidants to produce composite polypyrrole colloids. Palladium, platinum, and rhodium salts were suitable oxidants, producing polypyrrole in less than 12 h. © 2001 The Electrochemical Society. [DOI: 10.1149/1.1405802] All rights reserved.

Manuscript submitted April 13, 2001; revised manuscript received June 28, 2001. Available electronically September 21, 2001.

Methods for the preparation of colloidal gold have been known for hundreds of years.¹ Over this time, colloidal metals have found applications in biochemistry,² cytology,³ microscopy,⁴ and catalysis⁵ as described in recent reviews. Most of the procedures used to prepare colloidal metals rely on micelles as a stabilizer containing either metal salts or a reductant, thereby acting as microreactors to control the size distribution of the metal particles produced. The various morphologies that can be produced by this method have been described as “cherries” (one central metal particle), “raspberries” (multiple internal particles), “strawberries” (a layer of metal particles outside the micelle boundary), and “red currant” or “ginger root” (a dendritic type with strings of metal particles radiating away from the central micelle).⁶

Under conditions in which the reductant is a monomer that undergoes oxidative polymerization, a polymer/metal composite colloid can be formed. These are unique materials, with interesting electronic,⁷ magnetic,^{8,9} optical,¹⁰ and nonlinear optical properties,¹¹ depending on the metal and polymer employed. The metal thus supported can also be catalytically^{6,12,13} or electrochemically¹⁴⁻¹⁶ useful, especially with a conducting polymer as part of the system. Especially in terms of catalysis, polymer-supported precious metals have many applications. For example, polymer-supported platinum and rhodium catalysts have been used to carry out hydrogenation reactions.¹² The polymer allows the control of the environment around the metal center, thus influencing selectivity of the hydrogenation reaction.^{17,18} In terms of engineering applications, conducting polymer-supported catalysts are attractive materials for fuel cell design. For example, direct alcohol¹⁹ and proton exchange membrane cell²⁰ electrocatalysts based on conducting polymers have been studied.

Gold/polypyrrole composites have been prepared using both solution-phase and vapor-phase polymerization in inverse micelles in toluene.²¹ The stabilizer used in this case was a block copolymer [polystyrene-*block*-poly(2-vinyl pyridine)] and produced polypyrrole-coated gold particles in spherical, cubic, tetrahedral, and octahedral shapes in solution phase and dendritic particles from the gas-phase monomer. The micelle, in this case, acts as a microreactor and the particle morphology is partially constrained by the phase behavior of the surfactant system used. In the work cited, deviations from well-controlled, spherical particle distributions reportedly occurred around 13 nm, due to swelling of the reversed micelles by

pyrrole monomer. In addition, the nanoparticles thus produced are surrounded by a shell of polypyrrole. In the aqueous system used in our work, the colloidal gold is produced either as small (13 nm) or large (407 nm) particles supported on a polypyrrole matrix. A mixture of small and large particles is also theoretically possible if an excess of chlorauric acid is used.

The literature gives several accounts of the ability of polymers to act as reducing agents for metals in solution. For example it has been reported that chlorauric acid (HAuCl_4) can be reduced by sheets of polypyrrole^{22,23} and polyethylene oxide-polyethyleneimine block copolymer.²⁴ In the latter case, the oxidation of nitrogens in the polyimine polymer accompanies the reduction of chlorauric acid to metallic gold.

The production of polypyrrole colloids from aqueous²⁵ and nonaqueous²⁶ media is also well known. For example, the oxidation of the pyrrole monomer can be carried out rapidly using ferric chloride, which has been used for many years as an agent for preparing “pyrrole blacks” (suspensions of pyrrole polymer particles) in solution.²⁷ The mechanism of this reaction is shown in Fig. 1 and involves a one-electron oxidation of the pyrrole monomer to generate a radical cation. Two such radicals react to form a bond linking the two pyrrole rings. Subsequent loss of two protons yields an overall two-proton, two-electron oxidation.²⁸ The formation of the polymer is favored by the fact that the oxidation potentials of the *n*-mers decreases from +1.30 V vs. SCE for the monomer to -0.10 V vs. SCE for the bulk polymer.^{29,30} The polymer particles produced in this fashion may be either spherical³¹ or irregular.³² The formal potentials of the various oxidants used in this study are shown in Fig. 2.³³⁻³⁵ The redox potentials of pyrrole and its oligomers are shown for comparison.

Our goal is to investigate methods of producing polypyrrole/noble metal colloids. Due to the previously cited reactivity of polypyrrole with chlorauric acid, polypyrrole/gold composite colloids were chosen as our model system. If these methods can be generalized to other polypyrrole/noble metal colloids, these materials may find an application as catalysts.

In this study, we used preformed polypyrrole colloid, generated by reacting the monomer with ferric chloride in a sodium dodecylbenzenesulfonate (SDBS) solution, to subsequently reduce chlorauric acid. The particle size distribution and morphology of the resulting gold particles and polymer matrix has been characterized using transmission electron microscopy (TEM). In order to verify that the polymer was reducing the gold salt in solution, we used X-ray photoelectron spectroscopy (XPS) to probe the oxidation states of polypyrrole.³⁶ Energy dispersed X-ray analysis (EDS) detected the

^a Present address: Molecular Materials Research Center, Beckman Institute, California Institute of Technology, Pasadena, CA 91125.

^z E-mail: msf@caltech.edu

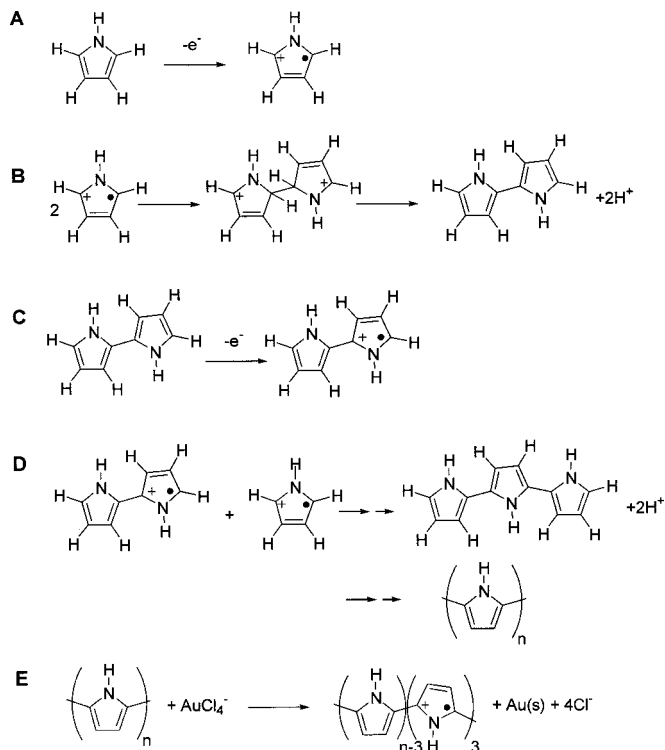


Figure 1. Reaction mechanisms for the oxidation of pyrrole and polypyrrole by chlorauric acid: (A) formation of radical cation, (B) coupling of radical cations and elimination of two protons, (C) formation of dimer radical cation, (D) chain propagation, (E) polymer oxidation by HAuCl_4 .

presence of gold, but could not give speciation information. Electron diffraction images provide additional evidence of the formation of metallic gold.

Chlorauric acid was also reacted with pyrrole monomer under conditions similar to those used to produce polypyrrole colloids with ferric chloride, with the oxidant being present in slight excess in both cases. The particles produced were characterized using the same techniques as the colloids produced in the first part of the study. We also examined the gold particles closely to determine if the particles produced differ from those reported for the inverse micelle system of Selvan and co-workers.²¹ Since chlorauric acid has a chromophore that absorbs in the ultraviolet region,³⁷ and polypyrrole has an absorbance in the visible region,³⁸ the rate constant

for the reaction between pyrrole and chlorauric acid in dilute solutions was determined by ultraviolet-visible spectroscopy and compared to that reported for ferric chloride.

In an additional experiment, we conducted a screening test to determine if other metals are capable of producing a polypyrrole colloid in aqueous solution. Palladium, platinum, rhodium, cobalt, tin, silver, zinc, nickel, titanium, cadmium, mercury, arsenic, and selenium were examined as potential oxidants. Palladium, rhodium, and platinum worked as oxidants, producing a polypyrrole black in 12 h or less.

Experimental

Reagents.—Pyrrole (Avocado Chemical) was distilled over zinc dust prior to use. Solutions of pyrrole were either used immediately, or stored under nitrogen and refrigerated in the dark. Chlorauric acid (HAuCl_4) and palladium chloride were used as received from Aldrich. Potassium hexachloroplatinate was used as received from Acros. Sodium dodecylbenzene sulfonate (SDBS) was used as obtained from Aldrich. Ferric chloride and hydrochloric acid (ACS grade) were used as received from Fischer scientific. Palladium(II) chloride, platinum(II) chloride, rhodium(III) chloride, cobalt(II) nitrate, tin(II) chloride, silver(I) nitrate, zinc(II) chloride, nickel(II) nitrate, titanium(III) fluoride, cadmium(II) nitrate, mercury(II) nitrate, arsenic(III) nitrate, and selenium(IV) nitrate atomic absorption (AA) standard solutions (1000 mg/L) were used as obtained from Fisher Scientific. The standards also contained *ca.* 5% HNO_3 , HCl , or HF stabilizer as appropriate.

Preparation of polypyrrole colloids with ferric chloride.—Polypyrrole colloids were prepared as follows, based on the method of Armes and co-workers,²⁵ with concentrations and surfactant modified as indicated. The polypyrrole colloid was made by adding 1.6 mL of a 10% (w/w) solution of pyrrole in 0.5 M HCl and 24.0 mL of a 5% (w/v) solution of SDBS in 0.5 M HCl , to 48.0 mL of 0.5 M HCl in a 250 mL Erlenmeyer flask. A total volume of 1.6 mL of a 455 g/L ferric chloride solution was then added dropwise using a syringe over a 5 min period, while stirring on a magnetic stir plate. The mole ratio was 2:1, and there was 1 equiv pyrrole for 1 equiv ferric chloride. The solution reached a uniform black color within 1 h, however stirring was continued overnight to ensure complete reaction. Occasionally, flocculation was observed on the addition of the ferric chloride, but disappeared on stirring. This may have been due to the formation of the less soluble ferric dodecylbenzene sulfonate from the reaction of SDBS and some of the ferric chloride. A gelatinous brown layer in the centrifuged product was attributed to the formation of $\text{Fe}(\text{DBS})_3$, consistent with previous reports.³⁹

The colloidal polypyrrole produced by the above method was subjected to multiple wash steps to remove any residual ferric and ferrous chloride. The sample was placed in several 14×89 mm polyallomer ultracentrifuge tubes and spun at 70,000g in a Beckman ultracentrifuge at 25°C for 30 min. The clear supernatant was decanted, and the pellet was resuspended in deionized (DI) water by shaking and ultrasonication. The solution was washed twice in this manner to remove FeCl_2 , unreacted FeCl_3 , and SDBS. At this point, the density and viscosity of the solution were sufficiently low to allow the samples to be spun in a bench-top centrifuge for 1 h at 5000g. The pellet was treated three more times by adding 1 mL of a 10% (w/w) KCl solution to help remove excess surfactant. The sample tube was then filled with DI water, and the sample was resuspended and centrifuged. The theoretical yield is 12 mg, and a single reaction typically gave 8–10 mg of product. The actual yield is undoubtedly lower because this makes no allowance for doping of the polymer by the HCl solution, counterions, or adsorbed surfactant. The other colloid systems gave similar yields.

Preparation of polypyrrole/gold colloids by reacting polypyrrole colloids with chlorauric acid.—The washed sample, prepared as described above, was resuspended in 24 mL of 5.0% SDBS in 0.5 M

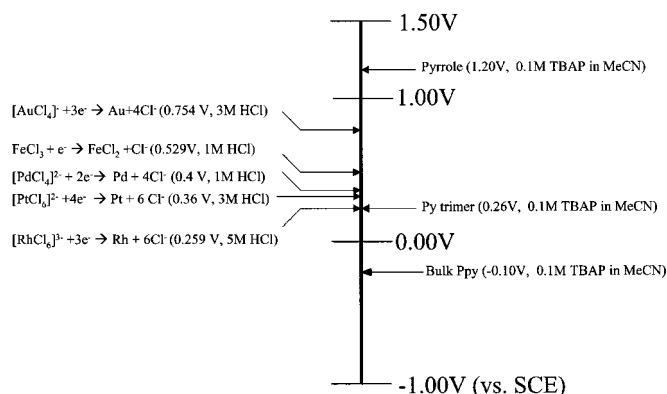


Figure 2. Formal potentials of pyrrole, pyrrole trimer, and the various oxidants used to produce colloids in this study. All values are reported vs. SCE in HCl (concentration as noted).

HCl, and 48 mL of 300 mg/L HAuCl₄ solution in 0.5 M HCl was added and stirred overnight using a magnetic stir plate. The sample was again centrifuged and washed, using the protocol described above.

Preparation of polypyrrole/gold colloids by reacting pyrrole with chlorauric acid.—The samples prepared using chlorauric acid as an oxidant were synthesized as follows. 1.6 mL of a 10% solution of pyrrole in 0.5 M HCl and 24.0 mL 5% SDBS in 0.5 M HCl, were added to a 250 mL Erlenmeyer flask. 48.0 mL of a 300 mg/L HAuCl₄ solution in 0.5 M HCl was added dropwise over a 5 min period with stirring. The mole ratio of pyrrole to HAuCl₄ was 50:1, and there was a ratio of 33 equiv pyrrole to each equivalent of HAuCl₄. The solution was stirred overnight. The solution was centrifuged using the protocol described above to produce the final washed sample. No gelatinous precipitate was observed for these samples, so sample clean-up was considerably easier.

Preparation of polypyrrole/metal colloids by reacting pyrrole with Pd, Pt, and Rh metal salts.—Solutions were prepared as described above, except that the oxidant was changed as follows. For palladium, 48.0 mL of a 235 mg/L solution of PdCl₂ in 0.5 M HCl was used (mole ratio 35:1, equivalence ratio 35:1). The platinum solution was 48.0 mL of 321.7 mg/L solution of potassium hexachloroplatinate in 0.5 M HCl (mole ratio 71:1, equivalence ratio 36:1). The rhodium colloid was prepared from 4.36 mL of a commercial 1000 ppm RhCl₃ standard solution and 43.6 mL of 0.5 M HCl (mole ratio 53:1, equivalence ratio 35:1).

Transmission electron microscopy (TEM).—Samples were ultracentrifuged (1/2 h at 70,000g), dried overnight, and then resuspended by ultrasonication in chloroform, followed by dilution to a ca. 5% solution. The samples were dispersed on carbon-coated copper TEM grids (Ted Pella, Inc.). Grids can be damaged by the rapid evaporation of a large amount of solvent. To avoid this, a single drop was placed on the grid, and the excess solvent was removed by capillary action by touching a corner of a laboratory wipe to the grid edge. The TEM used was a Philips FEI 400T equipped with an Oxford Link energy dispersed spectrum (EDS) X-ray analyzer.

Particle size analysis.—Particle size analysis was carried out on a Coulter N4MD particle size analyzer. Sample colloids were diluted with Nanopure deionized water until the instrument indicated that the count rate was low enough to permit analysis. The samples were measured in 1 cm disposable polystyrene cuvettes. The instrument was operated in the simultaneous data processing mode to permit the analysis of multimodal particle size distributions. The analysis was performed at 25°C, the solution viscosity was set to 0.0089 P, and a refractive index of 1.333 was assumed for the solution.

The particle size was also determined from the TEM. The NIH Image V1.59 program (National Institutes of Health, Bethesda, MD, USA) was used to determine the dimensions of the particles from the TEM images. Since the particles of interest are nearly spherical, the maximum particle dimension was taken as the diameter of the particle. Particles touching the edge of the image were rejected from the count.

X-ray photoelectron spectroscopy (XPS).—XPS measurements were obtained using a Scienta ESCA 300, with a monochromatic source consisting of an Al K α line at 1486 eV from a rotating anode operating at 1.0 kW. Analyses were performed at a photoelectron takeoff angle of 90° relative to the sample surface with an analyzer pass voltage of 150 eV. The centrifuged and dried pellet, prepared as described in the TEM section above, was crushed and applied to a carbon tape backing on a sample stud and placed in the instrument.

A survey scan was obtained from 5–1100 eV (one sweep at 0.991 eV/step). High-resolution measurements were also performed in the gold 4f region from 80–92 eV (five sweeps at 0.0499 eV/step), the nitrogen 1s region from 389–415 eV (four sweeps at 0.0498 eV/step), and the iron 2p_{3/2} region from 700–740 eV (two sweeps at

0.1990 eV/step). All curve fitting was performed using a Voigt distribution and a fixed linewidth. The data output of the instrument was corrected for relative sensitivities of the elements studied. The correction factors for the particular instrument were determined by the electron spectroscopy for chemical analysis (ESCA) facility staff and incorporated into the data analysis software.

UV-vis spectroscopy.—UV-vis spectroscopy was performed using a Shimadzu UV-2101 double beam spectrophotometer. The chlorauric acid concentration was followed at its absorbance maximum at 3.2 eV (315 nm). The formation of the polypyrrole was followed using its valence-to-conduction band transition absorbance at 1.5 eV (800 nm).^{29,38} The reaction was carried out by placing 1.0 mL of 0.05% (w/v) SDBS in 0.5 M HCl solution and 1.0 mL of 100 mg/L chlorauric acid in 0.5 M HCl in 1 cm quartz cuvette. A volume of 36 μ L of a 1% (w/v) pyrrole solution in water was added to initiate the reaction. The sample was mixed by inversion, and placed in the beam path in a thermostated cuvette holder set to 25°C. Readings were taken four times per second for 5 min vs. a 0.025% SDBS in 0.5 M HCl blank. The reaction was run twice to collect data at both wavelengths.

This system was rerun using a 205.9 mg/L solution of ferric chloride in place of the chlorauric acid solution. Since the molar absorptivity of the ferric chloride solution was much lower than the molar absorptivity of the chlorauric acid, it was not possible to follow the change in ferric chloride concentration with time.

Rapid screen of potential oxidants.—1.0 mL of palladium(II) chloride, platinum(II) chloride, rhodium(III) chloride, cobalt(II) nitrate, tin(II) chloride, silver(I) nitrate, zinc(II) chloride, nickel(II) nitrate, titanium(III) fluoride, cadmium(II) nitrate, mercury(II) nitrate, arsenic(III) nitrate, and selenium(IV) nitrate atomic absorption standards were added to individual vials. 1.0 mL of a 1% solution of pyrrole in water was added to each vial, and the mixture was allowed to stand overnight. The samples were then visually examined for the formation of polypyrrole black.

Results and Discussion

TEM micrographs.—The oxidative polymerization of pyrrole has been achieved by using a variety of chemical oxidants.^{27,29} Through the addition of surfactants^{27,31,32} and block copolymers^{21,24} it is possible to generate colloidal suspensions of polypyrrole. Figure 3 shows the TEM micrographs obtained for the oxidative polymerization of pyrrole (30 mM) by chlorauric acid ($n = 3$, 0.5 mM) and ferric chloride ($n = 1$, 60 mM) under identical solution conditions (0.5 M HCl and 0.16% SDBS). The TEM results show that both reactions result in similar amorphous conducting polymer structures, however in the case where chlorauric acid is used, small clusters of metal particles, as evidenced by EDS analysis and XPS (see below), are observed as shown in Fig. 3A.

Figure 4A shows some of the gold particles produced under the conditions in Fig. 3A under higher magnification. Due to the small size of these particles, it was difficult to obtain clear diffraction patterns, however the spots observed in Fig. 4B suggest the presence of crystalline metal, where the presence of gold was indicated by EDS. EDS analysis did not indicate the presence of iron in any of the samples. Figure 3A shows some circular, dense areas within the polymer that are likely gold nanoparticles, or clusters of nanoparticles. However the only clear images of these gold particles were obtained from isolated clusters of metal particles located away from the larger polypyrrole particles.

In contrast, Fig. 5A shows the colloidal gold particles produced upon exposing 2.1 g/L colloidal polypyrrole (produced under the conditions described in Fig. 3B) to 1.5 mM HAuCl₄. These particles represent either large gold particles or the clustering of a number of smaller gold particles on top of the amorphous colloidal polypyrrole. They were always found in intimate contact with polymer. The nodular structure of these particles is similar to metals deposited on carbon and conducting polymer electrodes. In particular, the resemblance to platinum particles electrochemically grown on polyaniline

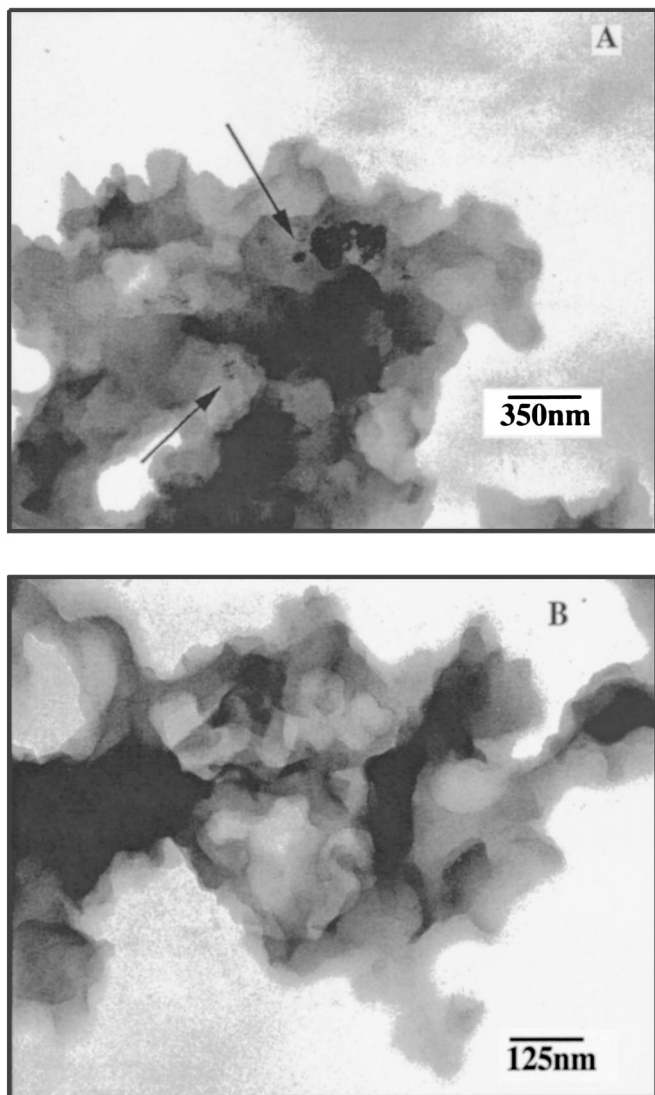


Figure 3. TEM images of polypyrrole produced by the oxidation of 3.0 mM pyrrole in 1.6% (w/v) SDBS/0.5 M HCl with (A) 0.5 mM chlorauric acid (28,000 times) and (B) 7.7 mM ferric chloride (80,000 times). Arrows indicate gold nanoparticles/clusters in the polymer matrix.

is striking.^{40,41} The large size of the particles made characterization by electron diffraction difficult, however the diffraction patterns could be observed from isolated bumps on the surface of the larger particles as shown in Fig. 5B. This morphology is in contrast to the previously reported rod-like structure at similar ratios of monomer to oxidant. However, the gold/polymer colloids reported by Selvan and co-workers²¹ were prepared in a system using a block copolymer in toluene in an inverse micelle system instead of SDBS in an aqueous system. Since the previous work relies on the inverse micelle to form a microreactor, the particle morphology is subject to greater control, but it may also be altered by the phase behavior of the micelle system. A given particle size/morphology combination may be impossible to produce due to the formation of nonspherical micelles at a given surfactant concentration. This effect can also be exploited, and the rod-like micelle phase of a cationic micelle system has been used to produce rod-like gold particles.⁴²

The system described by Selvan and co-workers has the unique property of producing gold particles surrounded by a shell of polypyrrole. The system described in this paper produces gold particles of various sizes exposed on the surface of a polypyrrole colloid. Our

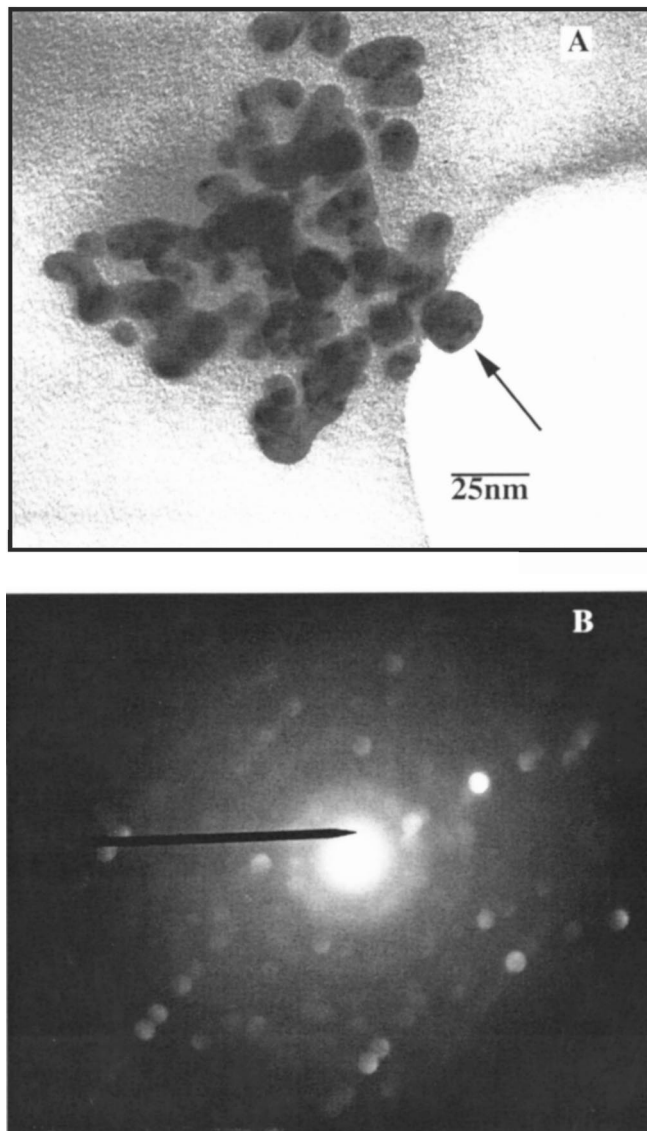


Figure 4. Gold particles produced by the oxidation of pyrrole by chlorauric acid under the conditions described in Fig. 3. (A) TEM image (410,000 times); (B) electron diffraction pattern obtained from the gold particle indicated by arrow in Fig. 4A.

system is also chemically simpler, using only a conventional surfactant instead of the block copolymers.

Particle size.—Table I shows the particle-size data obtained from light scattering experiments and from TEM micrographs. From the table it is evident that the light scattering measurements overlook the gold nanoparticles formed by the oxidation of pyrrole monomer by HAuCl_4 , reporting the larger, more numerous polypyrrole particles instead. The TEM images therefore provide a more reliable measure of the gold particle size. On the other hand, the polypyrrole particles are highly irregular and tend to clump when deposited on TEM grids. Since it was difficult to find an isolated particle for measurement with the TEM, light scattering gave a better estimation of the size of the polypyrrole colloid. Because of this difficulty, the TEM value shown in Table I for the ferric chloride-only sample represents a measurement performed on a single isolated particle (not shown).

UV spectroscopy.—Since the reaction of the chlorauric acid with the pyrrole monomer was rapid, it was possible to observe the change in concentration of the chlorauric acid as it was reduced by

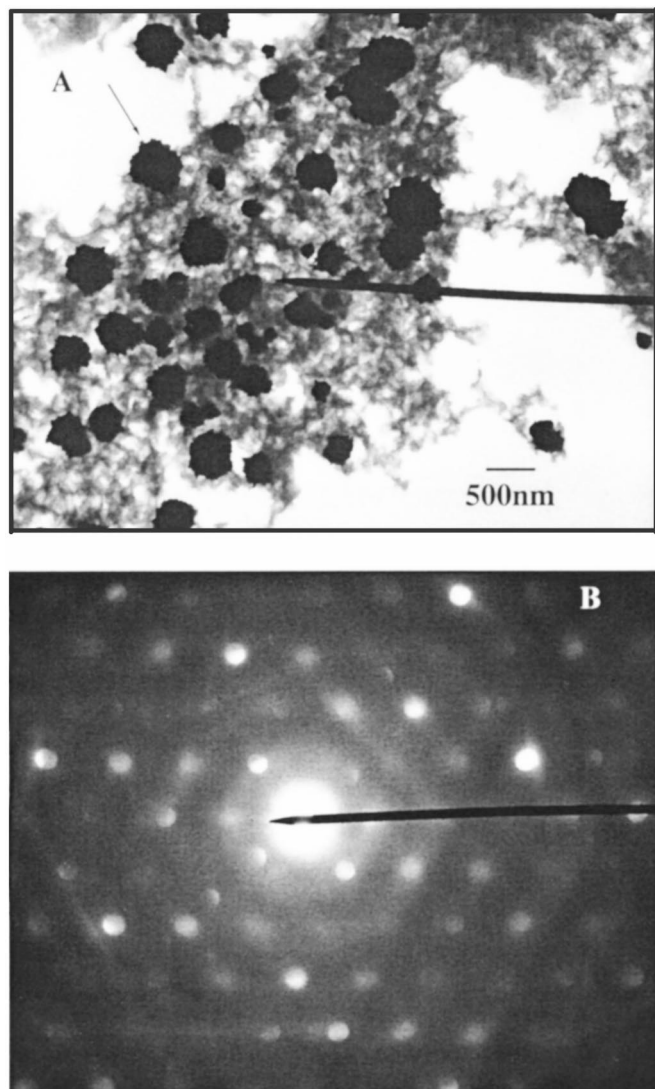


Figure 5. Colloidal gold particles on polypyrrole produced from the reduction of 0.5 mM chlorauric acid by 2100 mg/L colloidal polypyrrole in a 0.5 M HCl solution containing 1.6% SDBS as a surfactant. (A) TEM image (13,000 times); (B) electron diffraction pattern obtained from the gold particle indicated in Fig. 5A.

Table I. Particle size data for polypyrrole/gold colloids produced by oxidation of 30 mM pyrrole in a 0.5 M HCl solution containing 1.6% SDBS as a surfactant, using the oxidant(s) indicated. Oxidant concentrations were 0.5 mM for HAuCl_4 and 60 mM for FeCl_3 .

| Oxidation method | Particle size (nm) ^a | Particle size (nm) ^b |
|--------------------------------|---------------------------------|--|
| FeCl_3 | 413 ± 63 (PPy only) | 500 ± NA (<i>n</i> = 1) (PPy only) |
| HAuCl_4 | 368 ± 63 (Au&PPy) | 12.8 ± 9.4 (<i>n</i> = 27) (Au only) |
| $\text{FeCl}_3/\text{HAuCl}_4$ | 422 ± 35 (Au&PPy) | 407 ± 212 (<i>n</i> = 39) (Au only) |

^a Determined with dynamic light scattering measurements, tolerance ± 2 SD.

^b Determined from computer analysis of TEM micrographs, tolerance ± 2 SD.

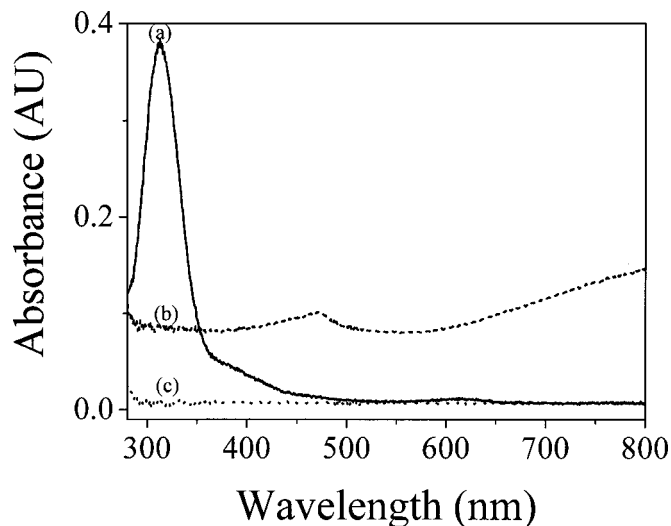


Figure 6. UV-vis spectra of pyrrole (1%), chlorauric acid (0.25 mM) (A), polypyrrole as formed (B), and pyrrole monomer (150 mM)(C).

the pyrrole by monitoring the absorbance at 3.1 eV (315 nm) (see Fig. 6). Under these experimental conditions, pyrrole, which had a minimum absorbance throughout the spectral range of interest, was present in excess. Therefore, the reaction was expected to be first order with respect to chlorauric acid. The spectra in Fig. 6 shows the absorbance of the reactants and the polypyrrole product following the reaction in dilute solution. Note the valence-to-conduction band transition at 1.5 eV (800 nm) and the $\pi \rightarrow \pi^*$ transition at 2.6 eV (477 nm), which is characteristic of polypyrrole.³⁸

Figure 7 shows the change in absorbance at 1.5 eV (800 nm) as a function of time associated with the loss of chlorauric acid and the generation of polypyrrole (due to the absorbance of the polymer and scattering associated with the colloid formed). The inset in Fig. 7 shows the pseudo-first order plot for the reaction during the beginning of the reaction where the spectra are dominated by chlorauric

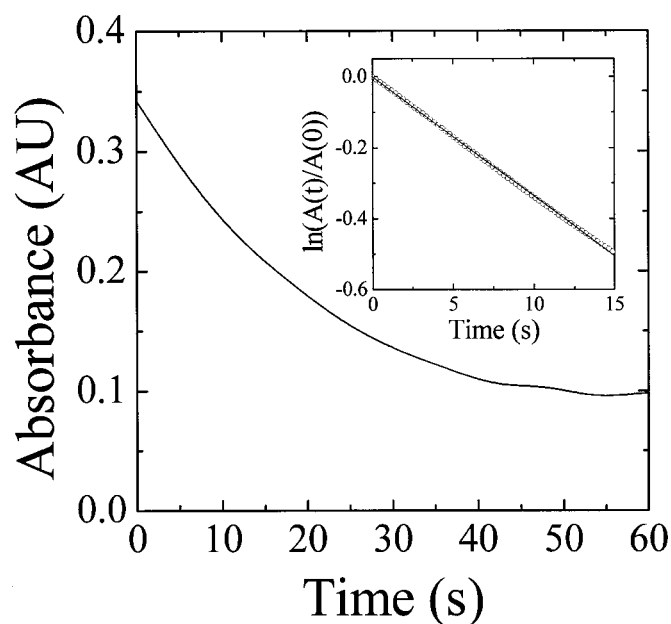


Figure 7. Time course of the formation of polypyrrole from pyrrole and HAuCl_4 in dilute solution. Inset: first-order plot for the oxidation of pyrrole by HAuCl_4 (0.13 mM).

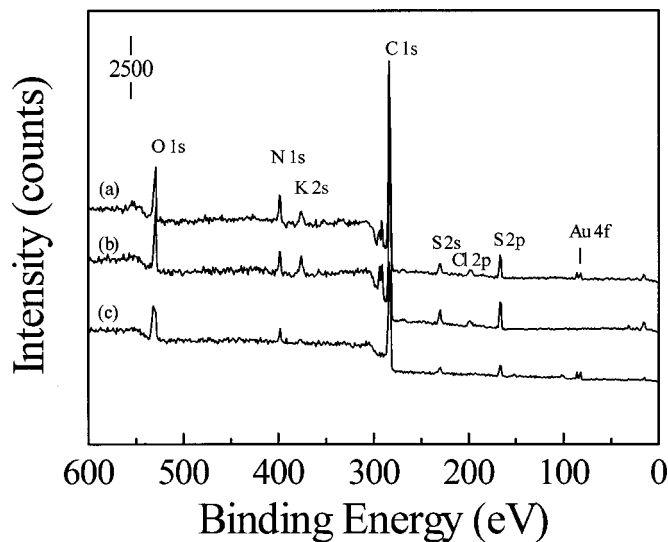


Figure 8. XPS survey scan of polypyrrole/gold colloids produced by oxidation of 30 mM pyrrole in a 0.5 M HCl solution containing 1.6% SDBS as a surfactant, using FeCl_3 (A), HAuCl_4 (B), and FeCl_3 followed by HAuCl_4 (C). Oxidant concentrations are 0.5 mM for HAuCl_4 and 60 mM for FeCl_3 . Spectra were taken from 0 to 1200 eV at a 90° takeoff angle with a 150 eV pass energy.

acid. The corresponding pseudo-first-order rate constant was determined to be 0.034 s^{-1} . Using the second-order rate equation

$$\text{Rate} = k[\text{HAuCl}_4][\text{Py}] \quad [1]$$

The pseudo-first-order rate constant (k') can be related to the second-order-rate constant (k) (under conditions where $[\text{Py}]_{\text{initial}} \approx [\text{Py}]_{\text{final}}$) by

$$k = k'/[\text{Py}] \quad [2]$$

For the 2.7 mM pyrrole solution used, a second-order rate constant of $13 \text{ M}^{-1} \text{ s}^{-1}$ was determined. This rate is considerably faster than that observed using ferric chloride ($0.01 \text{ M}^{-1} \text{ s}^{-1}$; in 0.3 M HCl)⁴³ or potassium persulfate (no rate was reported by the author for persulfate in aqueous solution, however the time-course data presented was similar to that cited for FeCl_3).⁴⁴ This difference is likely due to the higher standard potential of HAuCl_4 ($E^\circ = 0.754 \text{ V vs. SCE}$)⁴⁵ relative to FeCl_3 ($E^\circ = 0.529 \text{ V vs. SCE}$).³⁵ Persulfate has a higher oxidation potential ($E^\circ = 2.010 \text{ V vs. SCE}$),⁴⁶ however, it acts as both a free radical initiator and retarder thereby complicating the overall rate of polymerization.⁴⁷ The reactive intermediate is thought to be a sulfate radical^{45,48} rather than the persulfate ion itself, so the higher oxidation potential of persulfate may not directly influence the reaction rate.

X-ray photoelectron spectroscopy.—The XPS spectra support the evidence from electron diffraction and EDS data that the features observed in the TEM images are due to the presence of metallic gold. Figure 8 shows survey scans for colloids formed by the methods described in Fig. 3. The XPS spectra show that there is gold associated with the surface of the polypyrrole particles. Close examination of the iron region (not shown) indicates that there is no iron present to participate in a redox cycle with the chlorauric acid. It was therefore concluded that any oxidation of the preformed polypyrrole colloid upon exposure to chlorauric acid was due to the action of the chlorauric acid alone.

The survey scan also shows carbon and nitrogen from the polymer, potassium, and chlorine associated with residual KCl from the wash solution, and carbon, sulfur, and oxygen from the SDBS solution. Although residual SDBS is an insignificant part of the total

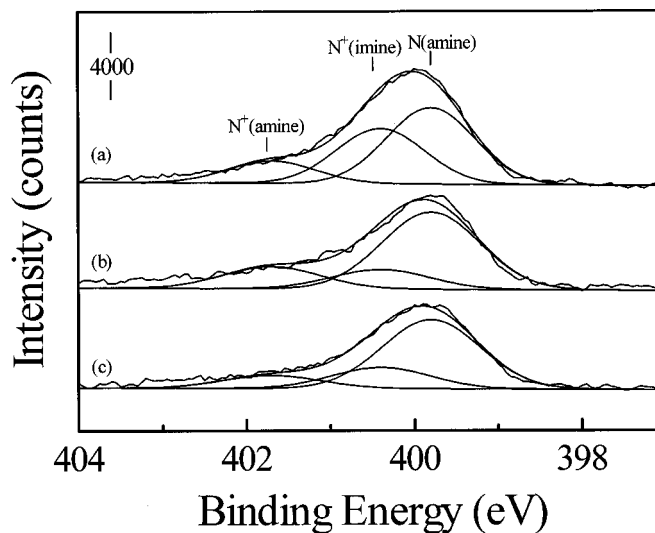


Figure 9. XPS spectra of the nitrogen 1s region of polypyrrole/gold colloids produced by oxidation of 30 mM pyrrole in a 0.5 M HCl solution containing 0.5% SDBS as a surfactant, using FeCl_3 (A), HAuCl_4 (B), and FeCl_3 followed by HAuCl_4 (C). Oxidant concentrations are 0.5 mM for HAuCl_4 and 60 mM for FeCl_3 . Spectra were taken from 398 to 415 eV at a 90° takeoff angle with a 120 mV pass energy.

weight of the sample, it is surface-active and is over represented in the XPS data. Figure 9 shows the high-resolution spectra of the nitrogen 1s region. The broad peak is an indication that nitrogen exists in several oxidation states. The observed spectrum could be fit with three peaks matching assignments previously reported for chemically oxidized pyrrole produced with ferric chloride.⁴⁹ These peaks include an amine nitrogen peak centered at 399.8 eV, a peak at 400.4 eV due to protonated imine nitrogens, and a peak at 401.7 eV due to protonated amine nitrogens.

As shown in Fig. 9, changes in the nitrogen 1s region illustrate a possible mechanism for the reduction of the gold from the oxidized to the metallic state. The samples of pyrrole oxidized with chlorauric acid and with ferric chloride show similar spectra, with a prominent peak for amine nitrogen and smaller peaks for imine and amine. However, when a chlorauric acid solution was applied to the preformed polymer, there was an increase in the relative peak area corresponding to the imine, indicating that it is the oxidation of nitrogen from an amine to an imine that provides the source of electrons for the reduction of the gold. A similar shift has been reported for the XPS spectra of polypyrrole sheets used to reduce chlorauric acid,²² however, the effect was less pronounced, probably due to the smaller surface-to-volume ratio of the sheet form of polypyrrole. Figure 10 shows the high resolution spectra obtained in the gold 4f region. The $4f_{5/2}/4f_{7/2}$ doublet at 88 and 84 eV for the pyrrole oxidized with chlorauric acid and for the chlorauric acid reduced by preformed polypyrrole colloids is consistent with the presence of metallic gold. The colloid sample formed by the oxidation of pyrrole with ferric chloride show no peaks in the gold region, as expected.

Table II shows the sensitivity-corrected absolute count rates obtained for the gold/polypyrrole colloids. The N 1s count rates of the three samples are of approximately equal magnitude, indicating that the amount of sample exposed to the beam in each sample is roughly equivalent. This data was used to calculate the relative count rates shown in Table III.

Examination of the relative count rates from the nitrogen 1s region and gold 4f region in Table III reveal several features. The relative amounts of amine, protonated amine, and protonated imine are similar for the samples oxidized with ferric chloride and chlorauric acid only. However, the sample in which the preformed poly-

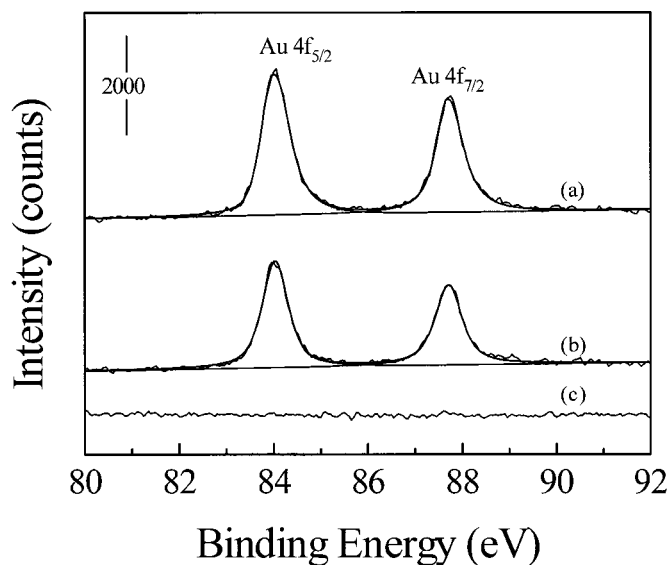


Figure 10. XPS spectra of the gold 4f region for polypyrrole/gold colloids produced by oxidation of 30 mM pyrrole in a 0.5 M HCl solution containing 0.5% SDBS as a surfactant, FeCl₃ (a), HAuCl₄ (b), and FeCl₃ followed by HAuCl₄ (c). Oxidant concentrations are 0.5 mM for HAuCl₄ and 60 mM for FeCl₃. Spectra were obtained at a 90° takeoff angle with a 120 mV pass energy.

pyrrole is oxidized by the chlorauric acid shows a decrease in the amine nitrogen counts and a concomitant increase in the imine ion peak. This change is expected since there is no more monomer available, and any oxidation that takes place must involve the existing polymer.

Based on the stoichiometry of the pyrrole polymerization reaction ($2e^-$, $2H^+$) and the valence of gold in chlorauric acid (3^+), a ratio of 3:2 for nitrogen to gold would be expected. In light of this, the observed ratio of 2:1 for nitrogen to gold is low in the polymer formed by reduction of HAuCl₄ by the monomer. This probably represents a surface effect, but it may also mean that some chlorauric acid is reduced only to the aurous (1^+) state and is removed in subsequent washing steps.

The ratio of gold to pyrrole nitrogens in the sample in which chlorauric acid is reduced by the preformed polypyrrole colloid is also consistent with the oxidation of a pyrrole nitrogen providing the electrons for reduction of the metal. The ratio of nitrogen counts to gold counts is 3.4:1. This ratio is low, but it is not less than the lowest possible ratio of 2:1 with one positive charge carried by two pyrrole rings in the polymer. Here again, the actual ratio is probably much higher. The gold is formed only at the surface of the polypyrrole, while the oxidized nitrogens may be either at the surface or deep in the polymer particle. This leads to an overestimation of the ratio of gold to nitrogen by XPS.

Screening of other potential oxidants.—Palladium(II) chloride, platinum(II) chloride, rhodium(III) chloride, cobalt(II) nitrate, tin(II)

Table III. Relative XPS intensities for various nitrogen oxidation states, expressed as a percentage of the total nitrogen counts, for polypyrrole/gold colloids produced by oxidation of 30 mM pyrrole in a 0.5 M HCl solution containing 1.6% SDBS as a surfactant, using the oxidant(s) indicated. Oxidant concentrations are 0.5 mM for HAuCl₄ and 60 mM for FeCl₃.

| Oxidation method | Amine N 1s (% total N cps) | Imine N ⁺ 1s (% total Ncps) | Amine N ⁺ 1s (% total Ncps) | Total gold (4f _{5/2} & 4f _{7/2}) (% total N cps) |
|---|----------------------------------|--|--|--|
| FeCl ₃ only | 66.8 | 20.5 | 12.6 | 0.0 |
| HAuCl ₄ only | 65.1 | 16.4 | 18.6 | 26.4 |
| FeCl ₃ , then HAuCl ₄ | 49.6 | 35.8 | 14.5 | 29.7 |

chloride, silver(I) nitrate, zinc(II) chloride, nickel(II) nitrate, titanium(III) fluoride, cadmium(II) nitrate, mercury(II) nitrate, arsenic(III) nitrate, and selenium(IV) nitrate were examined as potential oxidants for pyrrole. Palladium(II) chloride, platinum(II) chloride, rhodium(III) chloride were useful oxidants, producing a polypyrrole black in 12 h or less. The reactivity of the metals was as expected based on their oxidation potentials. The only unusual cases are silver and mercury, which have redox potentials higher than rhodium,⁴⁶ yet failed to produce a pyrrole black within the 12 h period. This is likely due to the fact that the reaction, although thermodynamically favorable, is kinetically very slow for these metals.

Detailed characterization of the colloids formed by platinum, palladium, and rhodium represent avenues for further research. Based on these results, platinum, palladium, and rhodium colloids were produced as described in the Experimental section and tested for catalytic activity.

Conclusions

We have shown that gold colloids can be produced in an aqueous solution via two different routes, using SDBS as a surfactant. These methods yield two different particle size regimes. In either case, the gold particles formed are accessible on the surface of the polymer colloid, instead of trapped within a polymer coating as they are when formed in an inverse micelle system.

Pyrrole can be oxidized by chlorauric acid, leading to the formation of polypyrrole particles with sizes on the order of 500 nm and metallic gold nanoparticles with sizes on the order of 13 nm. The gold particles have an irregular, amorphous structure associated with a porous matrix of larger polypyrrole particles. The gold particles produced are not coated with polypyrrole. If this technique is generally applicable to other noble metals these composite materials are potentially useful as catalysts. XPS, EDS, and electron diffraction confirm the presence of metallic gold, but we cannot rule out the possibility that some gold is only reduced to the aurous (1^+) state and removed by subsequent washing. This reaction has been observed in dilute solution and was shown to fit a second-order-rate law. The reaction proceeded with a rate constant of $13 \text{ M}^{-1} \text{ s}^{-1}$.

Platinum, palladium, and rhodium salts were shown to be capable of producing pyrrole blacks in aqueous solution. Colloids pro-

Table II. XPS count rates for gold and various oxidation states of nitrogen, corrected for relative sensitivity, for polypyrrole/gold colloids produced by oxidation of 30 mM pyrrole in a 1.5 M HCl solution containing 1.6% SDBS as a surfactant, using the oxidant(s) indicated. Oxidant concentrations are 1.5 mM for HAuCl₄ and 60 mM for FeCl₃.

| Oxidation method | Total N 1s (cps) | Amine N 1s (cps) | Imine N ⁺ 1s (cps) | Amine N ⁺ 1s (cps) | Total gold (4f _{5/2} & 4f _{7/2}) (cps) |
|---|---------------------|---------------------|----------------------------------|----------------------------------|---|
| FeCl ₃ only | 847 | 566 | 174 | 107 | 0 |
| HAuCl ₄ only | 970 | 631 | 159 | 180 | 256 |
| FeCl ₃ , then HAuCl ₄ | 1128 | 560 | 404 | 164 | 335 |

duced from these metals were screened for their ability to catalyze the hydrogenation of nitrobenzene. The palladium colloid was found to be catalytically active. The procedure described for gold may be generally applicable to the production of a wide variety of polypyrrole-supported precious metal catalysts. Preformed polypyrrole colloids can also reduce chlorauric acid in aqueous solution. Again, XPS, EDS, and electron diffraction confirm the presence of metallic gold. The gold particles produced by this method are relatively large (407 nm) and irregular, with a knobby, bumpy surface, similar to metals grown electrochemically. Theoretically, this technique could be combined with the formation of polymer by polypyrrole to give a mixture of large and small particle on the same polypyrrole support.

XPS analysis reveals that the oxidation state of the pyrrole nitrogens in the polypyrrole produced by oxidation with chlorauric acid is the same as in the pyrrole formed by oxidation with ferric chloride. When preformed polypyrrole colloids are used to reduce chlorauric acid, a shift from amine to imine nitrogen is observed, indicating that oxidation of the polypyrrole is responsible for the reduction of the chlorauric acid. Gold-to-nitrogen count ratios are consistent with the stoichiometry of the oxidative polymerization and polymer oxidation reactions.

Acknowledgments

The authors of this research paper acknowledge the allocation of time and services in the SCIENTA ESCA laboratory of Lehigh University. The technical assistance of Dr. Alfred C. Miller is greatly appreciated. We thank Dr. David Ackland of the Lehigh Electron Optics Laboratory for his advice and assistance in producing the TEM photomicrographs.

California Institute of Technology assisted in meeting the publication costs of this article.

References

1. D. Handley, *The Development and Application of Colloidal Gold as a Microscopic Probe in Colloidal Gold: Principles, Methods and Applications*, Vol. 1, M. A. Hayat, Editor, p. 1, Academic Press, Inc., New York (1989).
2. J. R. Thorpe, *Methods Mol. Biol.*, **117**, 99 (1999).
3. J. Chevalier, J. Yi, O. Michel, and X. M. Tang, *J. Histochem. Cytochem.*, **481**, 45 (1997).
4. W. Baschong and Y. D. Stierhof, *Microsc. Res. Tech.*, **42**, 66 (1998).
5. H. Boennemann, G. Braun, G. B. Brijoux, R. Brinkman, A. S. Tilling, K. Seevogel, and K. Siepen, *J. Organomet. Chem.*, **520**, 143 (1996).
6. A. Mayer, *Mater. Sci. Eng., C*, **6**, 155 (1998).
7. Y. Zwiefel, C. J. Plummer, and H. H. Kausch, *J. Mater. Sci.* **33**, 1715 (1998).
8. R. E. Partch, S. G. Gangolli, D. Owen, C. Ljungqvist, and E. Matijevic, *ACS Symp. Ser.*, **492**, 368 (1992).
9. S. R. Vadera, M. Parihar, S. C. Negi, and Kumar, in *Smart Materials, Structures, and MEMS*, V. K. Aatre and V. K. Varadan, Editors, Proc. SPIE Vol. 3321, p. 366, SPIE Int. Soc. for Opt. Eng. (1998).
10. A. H. Lu, G. H. Lu, A. M. Kessinger, and C. A. Foss, *J. Phys. Chem. B*, **101**, 9139 (1997).
11. M. P. Andrews, T. Kanigan, W. Xu, and M. G. Kuzyk, in *Photopolymer and Applications in Holography, Optical Data Storage, Optical Sensors, and Intercon-*
12. P. C. Selvaraj and V. Mahadevan, *J. Polym. Sci., Part A: Polym. Chem.*, **35**, 105 (1997).
13. C. W. Chen, T. Serizawa, and M. Akashi, *Chem. Mater.*, **11**, 1381 (1999).
14. F. Croce, G. B. Appetecchi, L. Persi, and B. Scrosati, *Nature (London)*, **456**, 6692 (1998).
15. I. Becerik and F. Kadirgan, *J. Electroanal. Chem.*, **436**, 189 (1997).
16. M. Somasundrum, M. Tanticharoen, and K. Krissnaphong, *J. Electroanal. Chem.*, **407**, 247 (1996).
17. A. B. Mayer and J. E. Mark, *J. Polym. Sci., Part A: Polym. Chem.*, **35**, 3151 (1997).
18. C. Lange, D. DeCaro, A. Gamez, S. Storck, J. S. Bradley, and W. F. Maier, *Langmuir*, **15**, 5333 (1999).
19. H. Laborde, A. Rezzouk, J. M. Leger, and C. Lamy, in *Electrode Materials and Processes for Energy Conversion and Storage*, S. Srinivasan, D. D. Macdonald, and A. C. Khandkar, Editors, PV 94-23, p. 275, The Electrochemical Society Proceedings Series, Pennington, NJ (1994).
20. S. Mukerjee and S. Srinivasan, *J. Electroanal. Chem.*, **357**, 201 (1993).
21. T. S. Selvan, H. Tomokatsu, M. Nogami, and M. Möller, *J. Phys. Chem. B*, **103**, 7441 (1999).
22. K. G. Neoh, T. T. Young, N. T. Looi, and E. T. Kang, *Chem. Mater.*, **9**, 2906 (1997).
23. E. T. Kang, Y. P. Ting, and K. L. Tan, *J. Appl. Polym. Sci.*, **53**, 1539 (1994).
24. L. M. Bronstein, S. N. Sidorov, A. Y. Gourkova, P. M. Valetsky, J. Hartmann, M. Breulmann, H. Cölfen, and M. Antonetti, *Inorg. Chim. Acta*, **280**, 1348 (1998).
25. S. P. Armes, M. Aldissi, G. C. Idzorek, P. W. Keaton, L. J. Rowton, G. L. Stradling, M. T. Collopy, and D. B. McColl, *J. Colloid Interface Sci.*, **141**, 119 (1991).
26. M. Beaman and S. P. Armes, *Colloid Polym. Sci.*, **70**, 271 (1993).
27. P. Praseti, *Chim. Italia*, **67**, 183 (1937).
28. C. P. Andrieux, P. Audebert, P. Hapiot, and J. M. Savéant, *J. Phys. Chem.*, **95**, 158 (1991).
29. M. S. Freund, C. Karp, and N. S. Lewis, *Inorg. Chim. Acta*, **240**, 447 (1995).
30. A. F. Diaz and J. Bargon, in *Handbook of Conducting Polymers*, Vol. 1, T. A. Skotheim, Editor, Chap. 3, Marcel Dekker Inc., New York (1986).
31. M. R. Simmons, P. A. Chaloner, and S. P. Armes, *Langmuir*, **14**, 611 (1998).
32. S. Y. Luk, W. Lineton, M. Keane, C. DeArmitt, and S. P. Armes, *J. Chem. Soc., Faraday Trans.*, **91**, 905 (1995).
33. *Encyclopedia of Electrochemistry of the Elements*, Vol. IV, A. J. Bard, Editor, p. 94, Marcel Dekker, Inc. New York (1975).
34. *Encyclopedia of Electrochemistry of the Elements*, Vol. VI, A. J. Bard, Editor, pp. 172, 255, 302, Marcel Dekker, Inc., New York (1975).
35. *Handbook of Chemistry*, 15th ed., J. A. Dean and J. A. Lange, Editors, p. 8-124, McGraw-Hill, New York (1999).
36. E. T. Kang, K. G. Neoh, and K. L. Tan, *Surf. Interface Anal.*, **19**, 33 (1992).
37. E. T. Kang, Y. P. Ting, K. G. Neoh, and K. L. Tan, *Polymer*, **34**, 4994 (1993).
38. K. Yakushi, L. J. Lauchlan, T. C. Clarke, and G. B. Street, *J. Chem. Phys.*, **79**, 4774 (1983).
39. M. P. Pileni, *Supramol. Sci.*, **5**, 321 (1998).
40. C. T. Hable and M. S. Wrighton, *Langmuir*, **9**, 3284 (1993).
41. C. T. Hable and M. S. Wrighton, *Langmuir*, **7**, 1305 (1991).
42. K. Esumi, K. Matsuhisa, and K. Torigoe, *Langmuir*, **11**, 3285 (1995).
43. M. M. Ayad, *J. Polym. Sci., Part A: Polym. Chem.*, **32**, 9 (1994).
44. M. M. Ayad, *J. Appl. Polym. Sci.*, **5**, 1331 (1994).
45. H. W. Starkweather, P. O. Bare, A. S. Carter, F. B. Hill, Jr., V. R. Hurka, C. J. Mighton, P. A. Sanders, H. W. Walkers, and M. A. Youker, *Ind. Eng. Chem.*, **39**, 1210 (1947).
46. P. Vanysec, in *CRC Handbook of Chemistry and Physics*, 71st ed, D. R. Lide, Editor, p. 8, CRC Press Inc., Boca Raton, FL (1990).
47. D. Balckley, *Emulsion Polymerization*, p. 155, Applied Science, London (1975).
48. F. A. Bovey, I. M. Kolthoff, A. I. Medalia, and E. J. Mechon, *Emulsion Polymerization*, p. 344, Interscience, New York (1955).
49. K. L. Tan, B. T. G. Tan, E. T. Kang, K. G. Neoh, and Y. K. Ong, *Phys. Rev. B*, **7563**, 42 (1990).